

Preparation and structure of novel siloxene nanosheets

Hideyuki Nakano,* Masahiko Ishii and Hiroshi Nakamura

Received (in Cambridge, UK) 19th January 2005, Accepted 14th April 2005

First published as an Advance Article on the web 29th April 2005

DOI: 10.1039/b500758e

We demonstrate the two-dimensional silicon backbone structure of siloxene nanosheets, which produces relatively monodisperse nanosheets with a thickness of 0.7 nm and lengths in the range 100–200 nm; the thickness is an order of magnitude smaller than that of previously reported silicon nanoparticles prepared by a variety of other methods.

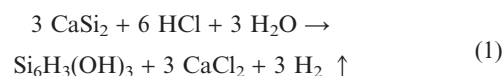
In the past decade, increased attention has been devoted to research on nanoscale materials because of their extraordinary structures, electronic and optical properties, and applications in nanodevices.¹ It is well known that certain clay minerals spontaneously undergo delamination in water to produce single-layer colloidal suspensions. It has recently been reported that similar exfoliation can be achieved artificially for several classes of layered materials by certain soft-chemistry procedures.² The exfoliation of the interlayer space, which occurs when layered materials accommodate guest species, modifies the interlayer which, at large interlayer expansions, may be weakened sufficiently for the layers to disperse completely. This extremely high anisotropy and a thickness of molecular dimensions are strikingly different from nanoparticles which generally have a spherical shape.³ Materials having a wide variety of compositions and structures have been synthesized using exfoliated nanosheets. For example, a layer-by-layer method has been utilized for the formation of more complex nanosystems using suspensions of layered materials.⁴

The conventional synthetic method of inducing exfoliation of layered materials, such as clay minerals,⁵ layered transition metal oxides,⁶ and phosphates,⁷ involves ion exchange of interlayer alkali metal ions with protons and the subsequent acid–base reaction of H-type materials with aqueous solutions of organoammonium ions.

Although exfoliation of layered materials has been widely studied, there have been no reports on non-oxide nanosheets. This communication, the first report on two-dimensional siloxene nanosheets, investigated the synthesis and properties of siloxene nanosheets, which are relatively monodispersed nanosheets with a thickness of 0.7 nm and lengths in the range of 100–200 nm. The thickness is an order of magnitude smaller than that previously reported for silicon nanomaterials with a silicon skeleton, such as silicon nanoparticles,⁸ silicon nanowires,⁹ and silicon nanotubes¹⁰ prepared by a variety of other methods.

The starting Weiss siloxene¹¹ $\text{Si}_6\text{H}_3(\text{OH})_3$ was synthesized by a topotactical reaction from the Zintl Phase CaSi_2 (Fig. 1(a)), a layered material with Si corrugated (111) layers linked by Ca ions. The structure of the siloxene depicted in Fig. 1(b) consists of Si (111) layers terminated above and below by OH groups and H

atoms.¹² The siloxene samples were prepared according to the method described by Weiss *et al.*¹¹ About 1 g of the selected CaSi_2 crystallites with 5-mm² faces was immersed in 100 ml of 37% HCl at 0 °C. The mixture was stirred continuously for 2 days under Ar atmosphere. During this process, the CaSi_2 transformed into a green-yellow solid and hydrogen gas was released via the following reaction:



After filtration and rinsing with EtOH, the Weiss siloxene $\text{Si}_6\text{H}_3(\text{OH})_3$ solid product was obtained. 0.0017 mol dm^{−3} sodium dodecylsulfate (SDS: $\text{C}_{12}\text{H}_{25}\text{OSO}_3\text{Na}$) (100 ml) was added into thin plate-like crystals of $\text{Si}_6\text{H}_3(\text{OH})_3$ (0.5 g) and then shaken (100 rpm) at R. T. for 10 days, which produced a translucent colloidal suspension. This suspension remained stable for 2 months, showing no precipitation. During exfoliation, hydrogen gas bubbling was observed. This means that the siloxene was slowly oxidized according to



Fig. 2 shows XRD patterns of the siloxene and colloidal aggregate centrifuged from the suspension. The broad reflection peaks of siloxene can be indexed on the basis of a hexagonal unit cell with $a = 0.383$ nm and $c = 0.63$ nm (Fig. 2(a)). The in-plane hexagonal lattice constant coincides with that of CaSi_2 ($a = 0.385$ nm), indicating that the reaction is topotactical and the two-dimensional silicon network of CaSi_2 is preserved. The diffraction

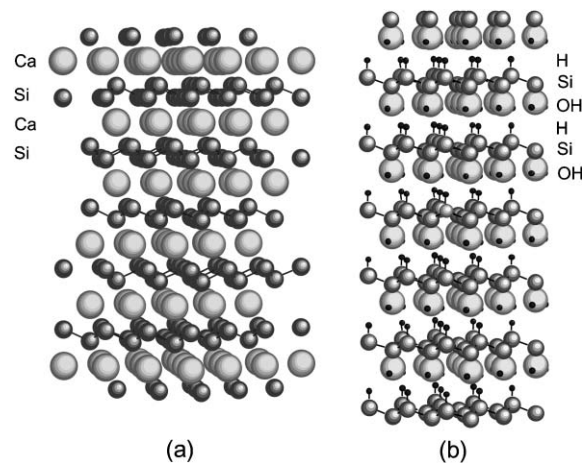


Fig. 1 Schematic illustration of (a) CaSi_2 and (b) Weiss siloxene $\text{Si}_6\text{H}_3(\text{OH})_3$.

*hnakano@mosk.tytlabs.co.jp

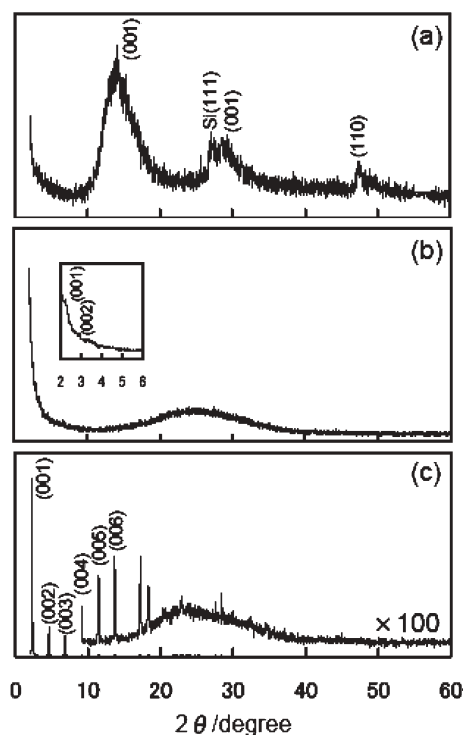


Fig. 2 XRD patterns before and after the exfoliation: (a) a polycrystalline sample of $\text{Si}_6\text{H}_3(\text{OH})_3$, (b) a wet colloidal aggregate and (c) a dried colloidal aggregate centrifuged from the exfoliated siloxene suspension for 1 h at 30 °C.

pattern for the wet colloidal aggregate is characterized by amorphouslike features (Fig. 2(b)), which should be interpreted as a combination of scattering from water and siloxene. Disappearance of the diffraction pattern in Fig. 2(a) confirms that the layered structure was collapsed. However, a pair of broad peaks was observed in the very low angle range (Fig. 2(b) inset). Their spacing was 4.0 and 2.0 nm, which means that these are assignable to 001 and 002 reflections, respectively. This can be explained by stacking of the nanosheets in the suspension. Thus, the XRD data presumably suggested that the parent siloxene was exfoliated into individual nanosheets, a small portion of which was stacked to give the small angle scattering. On drying, the diffraction pattern changed, signaling an amorphous to crystalline transition, as depicted in Fig. 2(c), in which sharp diffraction peaks attributable to a basal spacing of 3.8 nm were observed. This represents a large expansion from the original value of 0.63 nm for siloxene and can be identified as belonging to a DS intercalated compound. Sasaki *et al.* investigated the reassembling process of exfoliated titanate.¹³ They reported that the crystallites of titanate nanosheets started to grow in terms of stacking number, particularly under drying at low humidity, and that the final titanate nanosheets intercalated with TBA ions were accounted for by a sequence of fourteen or fifteen sheets. Our XRD data are very similar to the above phenomena, and it can be concluded that almost all of the siloxene nanosheets were restacked as a 10–20 sheet unit.

Fig. 3(a) shows a TEM image of siloxene nanosheets adsorbed on a carbon film, showing their general characteristics. The siloxene nanosheets had a lateral dimension of less than 200 nm.

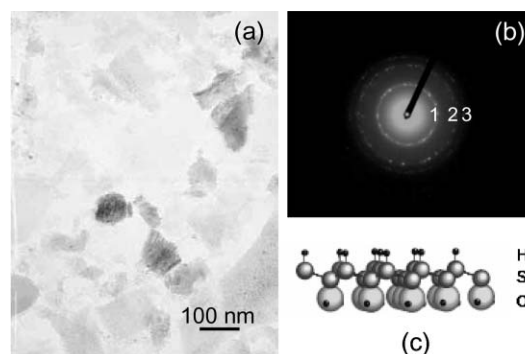


Fig. 3 (a) TEM image of siloxene nanosheets. (b) Electron diffraction pattern for the siloxene nanosheets. Indices and spacings for the diffraction rings 1–3 are (1) 10, 0.313 nm, (2) 11, 0.188 nm and (3) 20, 0.163 nm, respectively. (c) Schematic illustration of siloxene nanosheet.

The sheets were almost transparent, which indicated a high degree of exfoliation, and exhibited uniform and homogeneous contrast, reflecting their ultrathin nature and unit thickness. However, fragments were also observed in small quantities. It could be seen that cleavage occurred in many layers throughout the particle, rather than on a layer-by-layer basis starting from the surface. When exfoliation is completed, the particles are divided into a large number of ultrathin nanosheets. Evidence for preservation of the two-dimensional silicon network during exfoliation was provided by electron diffraction (Fig. 3(b)), taken with the electron beam along the [111] zone axis, perpendicular to the sheet surface. All the diffraction spots could be indexed as hk reflections for a two-dimensional hexagonal lattice with $a = 0.375$ nm, which is consistent with the structure of the parent Weiss siloxene. This indicated that the two-dimensional silicon network of siloxene was preserved. The architecture of the siloxene nanosheet is schematized in Fig. 3(c). The structure of the corrugated silicon layer is retained and the silicon atoms exhibit alternating Si–H and Si–OH bonds. On annealing at 900 °C in vacuum, the nanosheets changed into silicon crystals.

A tapping-mode AFM image (Fig. 4) of the sample adsorbed onto a mica substrate revealed two-dimensional structures with lateral dimensions similar to those detected by TEM. The nanosheet thickness was measured at steps between the nanosheets and the substrate surface, yielding average values of 0.7 nm, as shown in the roughness profile. The consistency in the thickness data and the fact that the thickness was below 1 nm clearly demonstrated that the sample was composed of nanosheets. These dimensions fell in the range of molecular species rather than small particles. The crystallographic thickness of the nanosheet was calculated to be 0.65 nm based on its atomic architecture. The close match between this value and that obtained by AFM indicated that the nanosheets consisted of single siloxene layers.

The colloidal suspension obtained by the procedures mentioned above was light yellow, depending on the parent siloxene. When the siloxene nanosheets dispersed in the aqueous suspension, Tyndall light scattering was observed. Fig. 5 depicts room-temperature absorption spectra for the nanosheet suspension. The data were characterized by Lambert–Beer behavior and a pronounced spectral blue shift. The former is represented in Fig. 5(b). The linear relationship indicates that the nanosheets were almost monodispersed. The absorption for the colloidal

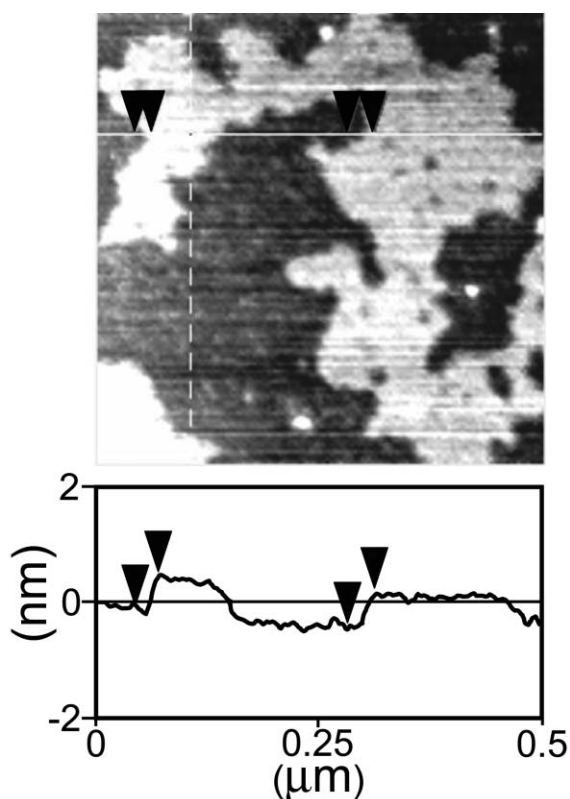


Fig. 4 Tapping mode AFM image of siloxene nanosheets.

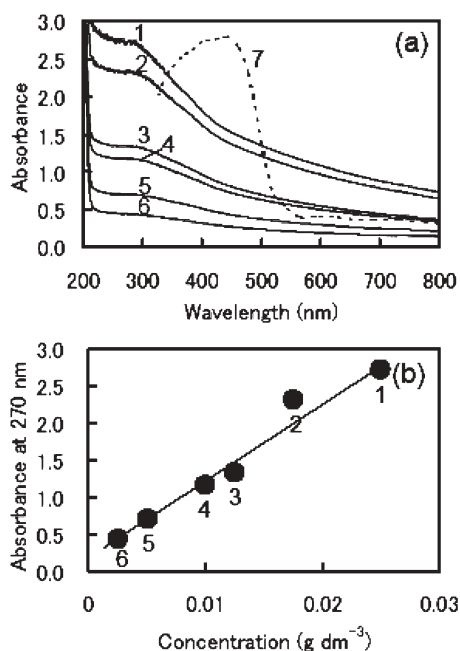


Fig. 5 (a) Optical absorption spectra of the colloidal suspension at various concentrations (1–6) and Weiss siloxene (7). The former were recorded in a diffuse reflectance mode and the latter in a transmission. (b) The absorbance at 300 nm as a function of the colloid content.

nanosheets was significantly blue shifted compared with those for bulk parent siloxene. Fig. 5(a) shows the diffusion reflectance spectrum for the parent siloxene together with the absorption

spectrum for the siloxene nanosheets. Although the different detection mode used to obtain the data makes a quantitative comparison difficult, the spectral change upon exfoliation is remarkable and may be associated with the disassembly of bulk crystals into nanosheets. Comparing the peak-top photon energy (4.6 eV) for the nanosheet with the band gap energy for bulk siloxene (2.4 eV), the energy shift of 2.2 eV is very large. Takeda *et al.* calculated the electronic structure of a two-dimensional silicon–oxygen high-molecular-weight polymer.¹⁴ They found that the oxygen position in the structure was very important in determining the band gap: if oxygen atoms are in the silicon skeleton backbone, the band gap is widened, whereas if oxygen atoms are located outside the silicon skeleton, the band gap is reduced. This is not the case for the present siloxene nanosheets because the silicon skeleton is preserved, as shown Fig. 3(b). This, along with the large energy shift, suggests that the spectral changes upon delamination are likely to be associated with size quantization.

In summary, we have prepared siloxene nanosheets by exfoliation of the Weiss siloxene. Preliminary near-UV absorption revealed quantum confinement effects in these nanosheets. Siloxene is interesting because it exhibits a strongly visible room-temperature luminescence, very similar to that of porous Si. Thus, research on the properties of nanosheets will likely yield results that will be of interest to nanotechnology.

Hideyuki Nakano,* Masahiko Ishii and Hiroshi Nakamura

Toyota Central R&D Labs., Inc., 41-1 Yokomichi, Nagakute, Aichi, 480-1192, Japan. E-mail: hnakano@mosk.tytlabs.co.jp

Notes and references

- 1 A. Bachold, P. Hadley, T. Nakanishi and C. Dekker, *Science*, 2001, **294**, 1317; Y. Huang, X. F. Duan, Y. Cui, L. J. Lauhon, K. H. Kim and C. M. Lieber, *Science*, 2001, **294**, 1313.
- 2 N. Miyamoto, H. Yamamoto, R. Kaito and K. Kuroda, *Chem. Commun.*, 2003, 2378; T. Sasaki and M. Watanabe, *J. Am. Chem. Soc.*, 1998, **120**, 4682; N. Yamamoto, T. Okuhara and T. Nakato, *J. Mater. Chem.*, 2001, **11**, 1858.
- 3 Y. Omomo, T. Sasaki, L. Wang and M. Watanabe, *J. Am. Chem. Soc.*, 2003, **125**, 3568.
- 4 R. S. Caruso, A. Susha and F. Caruso, *Chem. Mater.*, 2001, **13**, 400; Z. S. Wang, T. Sasaki, M. Muramatsu, Y. Ebina, T. Tanaka, L. Wang and M. Watanabe, *Chem. Mater.*, 2003, **15**, 807.
- 5 P. H. Nadeau, M. J. Wilson, W. J. McHardy and J. M. Tait, *Science*, 1984, **225**, 923.
- 6 K. Domen, Y. Ebina, S. Ikeda, A. Tanaka, J. N. Kondo and K. Maruya, *Catal. Today*, 1996, **28**, 264; R. E. Schaak and T. E. Mallouk, *Chem. Mater.*, 2002, **14**, 1455.
- 7 G. Alberti, S. Cavalaglio, C. Dionigi and F. Marmottini, *Langmuir*, 2000, **16**, 7663; N. Yamamoto, T. Okuhara and T. Nakato, *J. Mater. Chem.*, 2001, **11**, 1858.
- 8 R. D. Tilley, J. H. Warner, K. Yamamoto, I. Matsui and H. Fujimori, *Chem. Commun.*, 2005, 1833.
- 9 Y. Wu, J. Xiang, C. Yang, W. Lu and C. M. Lieber, *Nature*, 2004, **430**, 61; T. E. Bogat, S. Dey, K. K. Lew, S. E. Mohnney and J. M. Redwing, *Adv. Mater.*, 2005, **17**, 114.
- 10 J. Sha, J. Niu, X. Ma, J. Xu, X. Zhang, Q. Yang and D. Yang, *Adv. Mater.*, 2002, **14**, 1219; S. Y. Jeong, J. Y. Kim, H. D. Yang, B. N. Yoon, S. H. Choi, H. K. Kang, C. W. Yang and Y. H. Lee, *Adv. Mater.*, 2003, **15**, 1172.
- 11 A. Weiss, G. Beil and H. Z. Meyer, *Z. Naturforsch., Teil B*, 1979, **35**, 25.
- 12 J. R. Dahn, B. M. Way and E. Fuller, *Phys. Rev. B*, 1993, **48**, 17872.
- 13 T. Sasaki, M. Watanabe, H. Hashizume, H. Yamada and H. Nakazawa, *J. Am. Chem. Soc.*, 1996, **118**, 8329.
- 14 K. Takeda and K. Shiraishi, *Solid State Commun.*, 1993, **85**, 301.